UNIVERSITY OF AMSTERDAM

VRIJE UNIVERSITEIT AMSTERDAM

MSc Physics and Astronomy
Track: Astronomy & Astrophysics

Master Thesis

Title of Thesis

Subtitle of Thesis
Can use two lines

by

Karan Kumar
14906619(UVA)

December 4, 2024

60 ECTS

02-09-2024 - End date

Supervisors:
Lex Kaper
Daily Supervisor

Examiners
Alex De Koter

ANTON PANNEKOEK INSTITUTE

Contents

1 Introduction **1**

1.1 Introduction 1

1.1.1 Gaia DR3 1

1.1.2 History of HMXBs 2

1.1.3 Local Standard of Rest Frame 2

1.1.4 SuperNova Ejection Scenario 3

1.1.5 Dynamical Ejection Scenario 3

1.1.6 BeXray Binaries 3

1.1.7 The Compact Object 4

1.2 Tables 5

List of Figures

1.1 Local Standard of Rest Frame Delhaye (1965) 3

List of Tables

List of Abbreviations

Chapter 1

Introduction

1.1 Introduction

High mass X-ray binaries (HMXBs) consist of a massive star O-type or B-type ($\geq 8M_{\odot}$) orbiting a compact X-ray source. Typically a neutron star or black hole. The X-rays are produced via accretion from the massive companion either by stellar wind mass loss or by Roche-Lobe overflow van den Heuvel et al. (2000). Runaways are formed when the binary system is ejected out of the galactic mid-plane or if the system has high peculiar velocity. ($\geq$20-30 km/s) Although this velocity isn't constrained to this limit CITE CITE CITE. Since their prediction by Blaauw (1961) HMXBs have been observed through many space missions, the most significant being Hipparcos Chevalier & Ilovaisky (1998); Moffat et al. (1998) and *Gaia* Carretero-Castrillo et al. (2023) CITE APPELANIZ. My project it to use *Gaia* DR3 to search for HMXB runaways and measure their space velocity and reconstruct the evolutionary history of the binary system. Gaia Collaboration et al. (2023)

1.1.1 Gaia DR3

The *Gaia* space mission run by the European Space Agency provides astrometric solutions for the 3D position and velocity of stars in the galaxy with great precision. *Gaia* also classifies other parameters of stars such as effective temperature, metalicity and spectra. Since data release 3 (DR3) *Gaia* has mapped these parameters 1.8 billion sources with magnitudes as faint as G=21 and up to as bright as G=3 Gaia Collaboration et al. (2023).DR3 was released 13 June 2022 and publicly available on the *Gaia* archive, which let's users search for any star on the catalogue for free. The catalogue by Neumann et al. (2023) XRBcats contains the data for all known HMXBS in the galaxy for both the compact object and the optical counterpart. We use XRBcats to find the optical counterpart in the *Gaia* archive. For each optical counterpart we obtain the position, proper motions, parallax and radial velocities (if available) to determine the peculiar velocity of each star.

1.1.2 History of HMXBs

O Stars and B stars are the most massive hydrogen burning stars in the Milky Way Also known as population I stars, these stars are the youngest in the galaxy which makes them important to understand metalicity and supernovae and star formation, in the Milky Way these regions are localized to the spiral arms Neumann et al. (2023). these stars were significant in determining the Oort constant for differential rotation in the galaxy Gies & Bolton (1986). Among the O and B stars, there are a number of stars that have significantly high space velocity and move away from their OB association, their velocity cannot be explained by redshift (CITE GIES AND BOLTON 1987) therefore their space velocity must come from another mechanism. In Blaauw (1961) surveyed 19 O-type and B-type stars with space velocity greater than 40km s^{-1} and classified these stars as runaways. Following the work by Blaauw (1961) further results define runaways as stars with large peculiar velocity, Far distance from the the galactic mid-plane or a combination of both.(Blaauw (1961); Carretero-Castrillo et al. (2023); de Wit et al. (2005)). Of the observed O-type stars in the galaxy, 30% are runways GIES 1987

1.1.3 Local Standard of Rest Frame

Consider a star at point S as show in figure 1.1. point S is somewhere in the galactic plane, with distance R from the galactic centre. It has 3-component velocity (Π, Θ,z) Π represents the velocity component which is positive towards the galactic centre, $\vec{CS}$, Θ represents the velocity positive in the direction of galactic rotation and Z represent the velocity above the mid-plane. This represents the total velocity of the star at point S, for a given time. The total velocity is comprised of 1.The star's peculiar velocity, 2.the velocity due to galactic rotation 3.Observational bias from the sun's motion in the galaxy. If the galactic center rotates with velocity θ_c then we can reduce velocity of the star to it's local standard of rest frame (LSR) as

$$\vec{V_{lsr}} = [\Pi, \Theta - \Theta_c, Z]$$

Observationally, solar motion adds systematic error to the velocity since the sun is moving in the galactic plane as well, the true LSR velocity is therefore

$$\vec{V_{lsr}} = [\Pi - \Pi_{\odot}, \Theta - \Theta_c - \Theta_{\odot}, Z - Z_{\odot}]$$

Where $(\Pi_{\odot}, \Theta_{\odot}, Z_{\odot})$ represent the solar motion components. The peculiar velocity is always measured with respect to the LSR frame Delhaye (1965). All stellar motion is reduced to FROM SOLAR MOTION WHEN APPLICABLE (FIX)

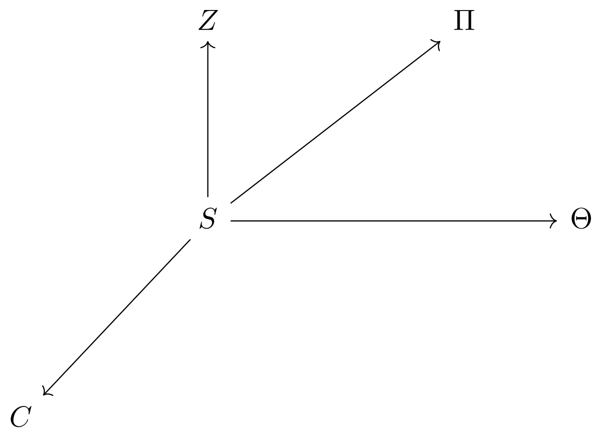

FIG. 1.1 – Local Standard of Rest Frame Delhaye (1965)

The Galactocentric distance is simply given by the law of cosine Brand & Blitz (1993), Moffat et al. (1998)

1.1.4 SuperNova Ejection Scenario

The compact object is a remenant of the most massive star in progenitor system called the primary star. As the more massive star it evolve much faster compared to the secondary star. During the core helium burning phase of the primary, the shell expands and mass transfer begins onto the primary via the secondary star Blaauw (1961), **?** At the end of it's lifetime the primary star allows explode into a Type II supernova becoming the compact the object.The roles are now switched the secondary now becomes the primary star in the system. The system can remain bound if less than half of the total mass of the system is lost during the supernova, CITE THIS. The energy of the supernova create the runaway velocity observed in HMXBs. van den Heuvel et al. (2000)

1.1.5 Dynamical Ejection Scenario

1.1.6 BeXray Binaries

Be X-Ray binaries consist of a compact object with a B-type emission companion star. Be-stars area a subgroup of B-type stars and are quite interesting to study as they have excited Balmer lines which generates emission Abt & Cardona (1984), Boubert & Evans (2018). Their emission comes from a circumstellar disk which is formed as a result of the rapid rotation of the Be-star around its axis Dufton et al. (2022). This circumstellar disk is also know as a deccretion disk which is also a source of infrared emissionCarretero-Castrillo et al. (2023). Be-stars may be a product of post-mass transfer systems Pols et al. (1991) in which a B-type star transfers mass into a companion, it is suggested that this post-mass transfer produces the deccretion disk in Be-stars therefore Be-stars may be a product of binary mass transfer, although the observational fraction of Be-stars in binary is poor Pols et al. (1991). This is paper THERE ARE N NUMBER OF Be-stars.

1.1.7 The Compact Object

Jeremy Orosz

1.2 Tables

	Name	l	b	distance	μ_l cos(b)	μ_b	V_{pec}	Mx	Mo
		deg	deg	kpc	mas/yr	mas/yr	Km/s	$M_\odot$	$M_\odot$
0.0	1A 0535+262	181.45	-2.64	1.91	2.13	-2.03	12.76	–	20.000000
1.0	1A 1118-61	292.5	-0.89	3.04	-5.57	-0.51	13.18	–	–
2.0	1E 1145.1-6141	295.49	-0.01	7.89	-6.61	0.83	49.26	1.7	14.000000
3.0	1ES 1210-64.6	298.89	-2.3	3.78	-5.96	-0.38	6.14	–	–
4.0	1FGL J1018.6-5856	284.35	-1.69	4.4	-6.65	-1.59	28.33	2.0	22.900000
5.0	1H 2202+501	97.25	-4.04	1.14	1.73	-1.64	24.95	–	–
6.0	1RXS J194211.9+255552	61.58	1.35	51.86	-4.43	-0.32	773.03	–	–
7.0	2MASS J20002185+3211232	68.99	1.13	14.82	-5.16	0.11	107.09	–	–
8.0	2RXP J130159.6-635806	304.09	-1.12	13.23	-6.31	-0.27	87.09	–	–
9.0	2S 0114+650	125.71	2.56	5.09	-1.32	0.62	20.31	–	16.000000
10.0	2S 1417-624	313.02	-1.6	11.91	-7.53	-1.83	141.1	–	–
11.0	3U 1223-62	300.1	-0.04	3.99	-5.03	-2.52	46.23	–	–
12.0	3U 1258-61	304.1	1.25	1.85	-4.35	-0.03	18.95	–	–
13.0	4U 0115+63	125.92	1.03	7.34	-1.73	0.31	21.92	–	–
14.0	4U 0352+309	163.08	-17.14	0.61	0.31	-2.25	14.03	–	–
15.0	4U 0728-25	240.28	-4.05	10.44	-1.99	0.09	9.27	–	–
16.0	4U 1145-619	295.61	-0.24	2.1	-6.43	0.1	8.98	–	–
17.0	4U 1538-52	327.42	2.16	7.81	-7.83	0.83	66.08	–	–
18.0	4U 1901+03	37.18	-1.25	2132.0	-4.67	-0.42	47012.0	–	–
19.0	4U 1907+09	43.74	0.48	4.3	-3.45	1.28	42.34	–	–
20.0	4U 1909+07	41.9	-0.81	1.92	-9.75	-0.87	56.9	–	32.000000
21.0	4U 1954+31	68.39	1.93	3.88	-6.3	-1.35	25.83	–	–
22.0	4U 2206+54	100.6	-1.11	3.28	-5.32	-0.32	26.16	–	–

23.0	AX J1700.2-4220	343.8	-0.03	1.56	-0.44	-1.83	18.07	–	14.600000
24.0	AX J1841.0-0536	26.76	-0.24	-14.31	-5.72	-0.64	-378.75	–	–
25.0	AX J1845.0-0433	28.14	-0.66	6.1	-5.6	-1.36	46.7	–	–
26.0	AX J1949.8+2534	62.14	-0.34	8.98	-5.64	-0.61	25.85	–	–
27.0	BSD 24-491	159.85	-1.27	2.64	0.96	-0.7	1.43	–	–
28.0	CCDM J07474-5320A	266.31	-13.73	0.65	-9.68	-0.05	4.8	–	–
29.0	Cen X-3	292.09	0.34	7.21	-3.72	1.16	85.15	1.34	20.200000
30.0	Cep X-4	99.01	3.31	9.54	-3.68	0.27	42.12	–	10.800000
31.0	Cir X-1	322.12	0.04	-8.03	-6.87	-0.39	-246.1	–	–
32.0	Cyg X-1	71.33	3.07	2.25	-7.37	-0.1	27.64	21.2	40.600000
33.0	EXO 2030+375	77.15	-1.24	2.93	-6.34	-0.55	19.26	–	17.500000
34.0	GRO J1008-57	283.0	-1.82	4.12	-5.89	0.25	13.02	–	17.500000
35.0	GRO J2058+42	83.57	-2.66	12.9	-3.97	-0.56	52.48	–	18.000000
36.0	Ginga 0834-430	262.02	-1.51	0.9	-4.95	-0.28	11.55	–	–
37.0	Ginga 1843+009	33.04	1.69	11.61	-4.42	-0.12	99.79	–	–
38.0	HD 110432	301.96	-0.2	0.44	-12.77	-3.98	1.78	–	–
39.0	HD 119682	309.16	-0.72	1.65	-5.13	-1.16	7.78	–	17.500000
40.0	HD 141926	326.98	-1.24	1.37	-4.46	-0.46	5.22	–	–
41.0	HD 153919	347.75	2.17	1.58	5.46	1.11	60.92	–	–
42.0	HD 161103	1.36	1.05	1.27	-2.41	-0.47	4.74	–	–
43.0	HD 215227	100.18	-12.4	2.06	-4.56	-1.13	10.3	–	–
44.0	HD 249179	181.28	1.86	1.67	2.21	-0.55	5.54	–	–
45.0	HD 34921	170.05	0.71	1.39	4.04	-1.18	12.13	–	–
46.0	HD 77581	263.06	3.93	2.02	-10.13	2.61	52.43	–	–
47.0	HD 96670	290.2	0.4	3.22	-6.88	-1.01	10.09	6.2	22.700000
48.0	HESS J0632+057	205.67	-1.44	1.85	0.37	-0.22	5.47	–	–

49.0	HR 4804	302.14	-12.52	0.21	-26.97	-9.99	7.2	–	–
50.0	IGR J00370+6122	121.22	-1.46	3.68	-1.82	-0.44	1.92	–	22.000000
51.0	IGR J01363+6610	127.39	3.73	5.99	-1.59	-0.32	9.42	–	12.500000
52.0	IGR J01583+6713	129.35	5.19	7.5	-1.23	-0.03	4.25	–	12.500000
53.0	IGR J06074+2205	188.39	0.81	7.24	0.81	0.2	23.13	–	14.600000
54.0	IGR J08262-3736	256.44	0.29	5.63	-3.96	-0.05	6.7	–	–
55.0	IGR J08408-4503	264.04	-1.95	2.26	-9.41	-2.08	40.72	–	33.000000
56.0	IGR J10101-5654	282.26	-0.67	7.54	-6.29	-0.57	41.74	–	–
57.0	IGR J11215-5952	291.89	1.07	8.11	-5.76	0.88	42.47	–	–
58.0	IGR J11305-6256	293.94	-1.49	1.74	-6.23	-0.49	7.02	–	17.500000
59.0	IGR J11435-6109	294.88	0.69	16.63	-6.22	-0.41	194.47	–	14.600000
60.0	IGR J12341-6143	300.87	1.08	71.51	-5.17	0.7	1424.98	–	–
61.0	IGR J14331-6112	314.85	-0.76	2.41	-8.23	-0.84	34.04	–	–
62.0	IGR J16195-4945	333.56	0.34	2.79	-0.51	-0.26	34.32	–	27.800000
63.0	IGR J16207-5129	332.46	-1.05	27.95	-7.71	-0.79	601.66	–	–
64.0	IGR J16318-4848	335.62	-0.45	-28.66	-7.2	-0.72	-982.26	–	–
65.0	IGR J16327-4940	335.06	-1.16	-36.59	-7.73	-0.64	-1343.49	–	–
66.0	IGR J16374-5043	334.8	-2.38	0.59	-2.66	-3.21	12.55	–	–
67.0	IGR J16418-4532	339.19	0.49	1.05	-9.62	2.96	34.97	–	–
68.0	IGR J16465-4507	340.05	0.14	3.38	-3.48	-0.63	18.82	–	27.800000
69.0	IGR J17200-3116	355.02	3.35	9.46	-6.38	1.0	131.99	–	–
70.0	IGR J17354-3255	355.46	-0.27	28.3	-10.05	-0.22	894.5	–	29.600000
71.0	IGR J17544-2619	3.24	-0.34	2.52	-0.83	0.1	9.44	1.4	23.000000
72.0	IGR J17586-2129	7.99	1.33	7.5	-4.48	0.15	66.77	–	–
73.0	IGR J18027-2016	9.42	1.04	-48.2	-6.45	0.25	-1484.41	1.5	20.000000
74.0	IGR J18048-1455	14.31	3.25	2.81	1.84	-2.2	47.79	–	–
75.0	IGR J18214-1318	17.68	0.49	8.94	-8.53	0.83	85.84	–	–

76.0	IGR J18406-0539	26.66	-0.23	4.3	-3.08	-0.45	3.22	–	–
77.0	IGR J18462-0223	30.22	0.08	1.48	-2.65	0.43	10.63	–	–
78.0	IGR J18483-0311	29.75	-0.75	2.72	-4.02	-0.18	18.16	–	–
79.0	IGR J19140+0951	44.3	-0.47	2.77	-5.62	-1.18	22.85	–	–
80.0	IGR J19294+1816	53.54	0.12	4.04	-5.16	0.67	20.43	–	12.500000
81.0	IGR J21343+4738	92.17	-3.12	11.97	-3.35	-0.43	30.81	–	–
82.0	IGR J22534+6243	109.92	2.86	16.75	-2.23	0.01	63.24	–	–
83.0	KS 1947+300	66.1	2.08	36.16	-4.67	-0.16	502.33	–	17.500000
84.0	LS 1698	285.35	1.43	5.84	-6.98	-0.4	32.74	–	–
85.0	LS 5039	16.88	-1.29	2.04	-3.73	-10.38	94.91	–	23.000000
86.0	LS 992	249.58	1.54	8.45	-2.59	-0.01	11.06	–	–
87.0	LS I +61 303	135.68	1.09	2.65	-0.28	-0.41	4.17	–	–
88.0	MAXI J0709-159	229.31	-3.36	3.17	-2.06	-0.99	10.59	–	–
89.0	MAXI J0903-531	273.08	-4.3	18.85	-3.02	0.06	46.73	–	–
90.0	MXB 0656-072	220.13	-1.77	6.5	-1.41	0.01	13.58	–	–
91.0	NGC 6649 9	21.64	-0.79	2.11	-0.09	-0.06	20.05	–	–
92.0	PSR B1259-63	304.18	-0.99	2.26	-7.1	0.04	12.99	–	22.500000
93.0	PSR J0635+0533	206.15	-1.04	7.02	-0.55	-0.18	10.19	–	–
94.0	PSR J2032+4127	80.22	1.03	1.76	-2.49	1.73	27.43	–	15.000000
95.0	RX J0146.9+6121	129.54	-0.8	3.05	-0.99	-0.31	4.52	–	9.600000
96.0	SAO 49725	85.23	5.05	2.38	-5.26	-0.51	8.06	–	–
97.0	SAX J1818.6-1703	14.08	-0.7	2.47	-4.79	-0.8	39.28	–	–
98.0	SAX J2103.5+4545	87.13	-0.68	7.64	-4.7	0.46	36.7	–	17.500000
99.0	SAX J2239.3+6116	107.73	2.36	9.62	-2.54	0.22	19.68	–	17.500000
100.0	SGR 0755-2933	246.23	-0.62	3.5	-3.86	-0.74	5.56	1.4	18.500000
101.0	SRGA J124404.1-632232	302.11	-0.52	8.11	-6.35	-0.42	15.15	–	–

102.0	SRGE J204319.0+443820	83.98	1.34	24.02	-4.94	-0.61	347.94	–	–
103.0	SS 397	21.47	-0.87	0.93	-0.1	-1.11	12.36	–	–
104.0	SS 433	39.69	-2.24	8.46	-5.64	0.45	31.01	4.2	11.300000
105.0	Sct X-1	24.34	0.07	–	–	–	–	–	–
106.0	Swift J0243.6+6124	135.93	1.43	5.51	-0.72	-0.19	2.38	–	–
107.0	Swift J1626.6-5156	332.78	-2.0	19.95	-4.38	-0.24	18.19	–	–
108.0	TYC 3681-695-1	126.08	-3.57	2.95	-2.39	-0.8	13.26	–	–
109.0	UCAC4 528-094936	49.0	2.75	-8.41	-5.53	-0.28	-166.25	–	–
110.0	V0332+53	146.05	-2.19	7.44	-0.48	0.2	18.23	–	–
111.0	XTE J0421+560	149.18	4.13	4.76	0.03	-0.7	10.76	–	–
112.0	XTE J1543-568	324.96	-1.46	-19.84	-4.89	0.5	-443.26	–	–
113.0	XTE J1739-302	358.07	0.45	1.94	2.96	2.36	50.5	–	33.700000
114.0	XTE J1743-363	353.37	-3.42	65.43	-3.74	2.97	1165.41	–	29.630000
115.0	XTE J1855-026	31.08	-2.09	12.86	-7.17	-0.87	82.9	–	–
116.0	XTE J1859+083	41.13	2.08	-10.99	-3.81	0.26	-158.04	–	12.500000
117.0	XTE J1906+090	42.5	1.17	3.05	-4.64	-1.44	15.97	–	–
118.0	XTE J1946+274	63.21	1.4	48.33	-4.71	0.02	766.04	–	15.000000
119.0	gam Cas	123.58	-2.15	–	–	–	–	–	13.000000
120.0	mu.02 Cru	303.36	5.7	0.12	-28.61	-9.82	3.28	–	–

Bibliography

Abt H. A., Cardona O., 1984, , 285, 190

Blaauw A., 1961, , 15, 265

Boubert D., Evans N. W., 2018, , 477, 5261

Brand J., Blitz L., 1993, , 275, 67

Carretero-Castrillo M., Ribó M., Paredes J. M., 2023, , 679, A109

Chevalier C., Ilovaisky S. A., 1998, , 330, 201

Delhaye J., 1965, in Blaauw A., Schmidt M., eds, , Galactic structure. Edited by Adriaan Blaauw and Maarten Schmidt.. University of Chicago Press, p. 61

Dufton P. L., Lennon D. J., Villaseñor J. I., Howarth I. D., Evans C. J., de Mink S. E., Sana H., Taylor W. D., 2022, , 512, 3331

Gaia Collaboration et al., 2023, , 674, A1

Gies D. R., Bolton C. T., 1986, , 61, 419

Moffat A. F. J., et al., 1998, , 331, 949

Neumann M., Avakyan A., Doroshenko V., Santangelo A., 2023, , 677, A134

Pols O. R., Cote J., Waters L. B. F. M., Heise J., 1991, , 241, 419

de Wit W. J., Testi L., Palla F., Zinnecker H., 2005, , 437, 247

van den Heuvel E. P. J., Portegies Zwart S. F., Bhattacharya D., Kaper L., 2000, , 364, 563